Wind Proofing LIGO

Elyssa Hofgard[1,2], Edgard Bonilla[1,2], Dr. Brian Lantz[1]
[1]*Stanford University, Ginzton Laboratory*
[2]*Stanford University, Department of Physics*

Interferometer Design and Noise Sources

LIGO's discovery of gravitational waves ushered in a new era of multi-messenger astronomy, confirming Einstein's theory of general relativity.

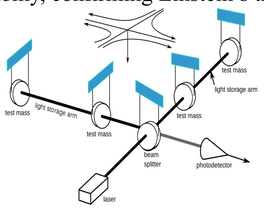

Figure 1. LIGO's interferometer.[1]

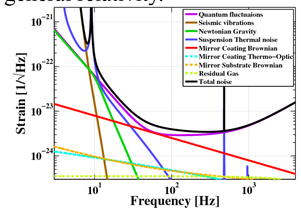

Figure 2. LIGO's noise budget.[2]

Wind at LIGO

LIGO employs both active and passive isolation to minimize seismic noise and to operate at high sensitivity. Horizontal tilt confuses LIGO's seismometers and can cause the system to execute spurious translations in response to low-frequency tilts, with the frequency response given by $\frac{-g}{\omega^2}$.[3] At LIGO Hanford, wind above 10 m/s causes a significant increase in tilt and occurs 15% of the time. To reduce problematic wind, LIGO has proposed building a fence around End Station X and End Station Y.

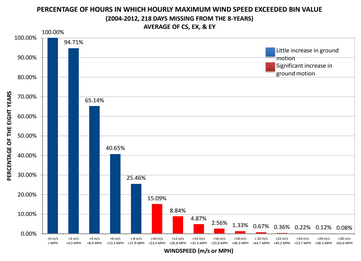

Figure 3. Maximum wind speeds.[4]

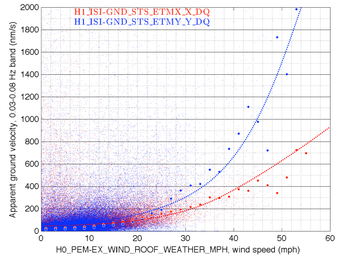

Figure 4. Ground tilt and wind correlation at EX and EY.[5]

Computational Fluid Dynamics (CFD) Modeling

k-ε CFD models are reasonably reliable for characterizing turbulent flow with high Reynolds numbers. k-ε models solve for turbulent kinetic energy or the root mean square velocity fluctuations (k) and the rate of dissipation of k (ε).

Design flow domain in SolidWorks → Mesh flow domain and optimize mesh parameters → Input boundary conditions and user defined functions → Initialize solution and run computation

Evaluating LIGO's Proposed Fence

Lab Measurements of Different Fence Materials
- Measured Tenax, Belton Industries, larger porosity material in a makeshift wind tunnel

Computational Fluid Dynamics (CFD) Modeling of End Station X and Fence
- Modeled fence as porous jump with k-ε numerical simulation

Model Validation Using Test Fence Data
- Installed and calibrate sensors at LIGO test fence
- Evaluated experimental data and verify CFD model

Results

1. Lab measurements of different fence materials => speed drop across porous material

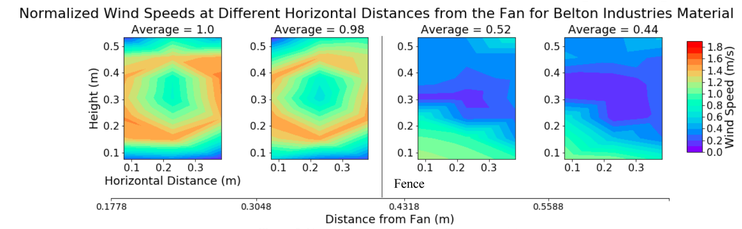

Figure 5. Normalized wind speeds for Belton material.

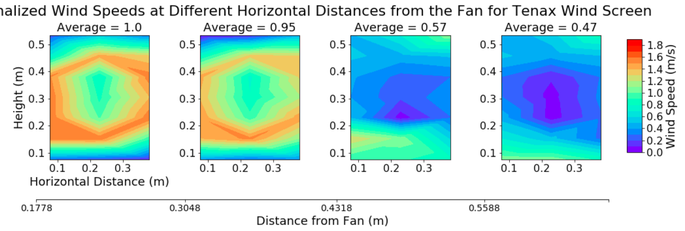

Figure 6. Normalized wind speeds for Tenax material.

2. CFD Results

RNG k-ε model with logarithmic velocity (v), logarithmic epsilon (ε), and porous jump Δp.

$v = \frac{u^*}{\kappa}\ln(\frac{z+z_0}{z_0})$, $\varepsilon = \frac{u^{*3}}{k(z+z_0)}$,[6] $\Delta p = -(\frac{\mu}{\alpha}v + C_2\frac{1}{2}\rho v^2)\Delta m$.[7]

u^*, κ = constants
z_0 = roughness height, .03
$\frac{\mu}{\alpha}v$ = viscous loss, negligible for turbulent flow, α = 1e+20 m
Δm = .01 m
C_2 = pressure loss coefficient related to porosity, 400 1/m for 50% porosity[8]

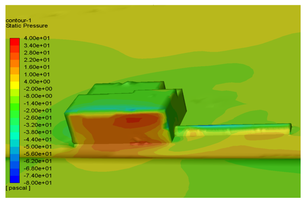

Figure 7. Static pressure on building logarithmic velocity without fence.

- Load on building 9217 N to 2197 N (76% reduction)
- Moment about y axis 28509 Nm to 4215 Nm (86% reduction)
- Velocity front of building 6.21 m/s to 3.19 m/s (49% reduction)

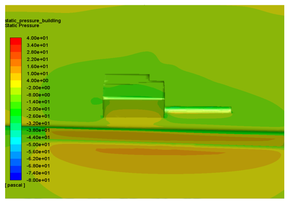

Figure 8. Static pressure on building logarithmic velocity with fence.

RNG k-ε model with 2x logarithmic velocity input

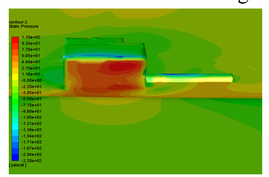

Figure 9. Static pressure on building double logarithmic velocity without fence.

- Load on building 34239 N to 9240 N (73% reduction)
- Moment about y axis 108634 Nm to 5393 Nm (95% reduction)
- Velocity front of building 11.12 m/s to 6.08 m/s (45% reduction)

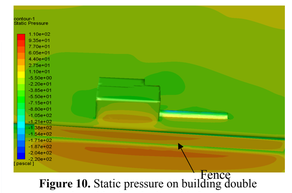

Figure 10. Static pressure on building double logarithmic velocity with fence.

3. LIGO Test Fence Data and Model Validation

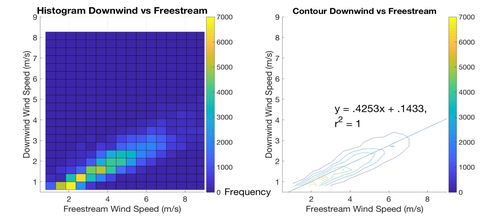

Figure 11. 2D histogram and contour of freestream sensor vs downwind sensor with a line of best fit for August 16-17. This shows about a 57% reduction in wind speed downwind.

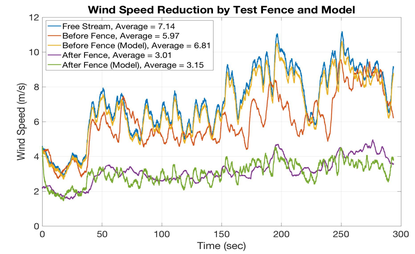

Figure 12. Time series for model and test fence data.

Steady State Model
RNG k-ε model with test fence, building, 12 ft cut in ground, logarithmic velocity profile. The model shows a 60% reduction in wind speed after the fence.

Table 1. Test fence and steady state model results.

Average Velocity	Test Fence (+/- .5 m/s)	Model
Freestream	4.36	5.83
Before Fence	3.65	3.05
After Fence	2.64	2.37
EX Roof	5.63	5.96

Transient Model
5 minutes of data 22:40-22:45 August 16, .0625 second time step (4,800 data points). The model shows more variability than the real data in some areas, suggesting that the fence may smooth wind flow.

Discussion and Further Steps

Both fence materials offer similar protection, so the main differences between Tenax and Belton will arise from cost and material strength. CFD model results demonstrate that a **50% porous fence is quite effective in reducing the load on the building**, which scales roughly as v^2. The velocity input is doubled to obtain the same loading with a porous fence. With a fence, problematic wind speeds could be > 20 m/s, which only occur 1.45% of the time (compared to 15% for wind > 10 m/s). The Tenax test fence at LIGO shows promising effects, **slowing wind speeds by 57%.** Data from the test fence agrees reasonably well with steady state and transient model results, assuaging fears about model reliability. **A 50% porous fence is a well-motivated wind proofing measure for End Station X.**
In the future, we will evaluate the real fence once it is installed at End X and build a fence at End Y. Transient modeling should also be further explored with the possibility of running Large Eddy Simulations (LES) to more accurately characterize turbulence and wind gusts. While these results are promising, they are preliminary. We will collect more experimental data to verify model accuracy.

Contact

Elyssa Hofgard
Stanford University
ehofgard@stanford.edu

Acknowledgements

I would like to thank Brian Lantz, Edgard Bonilla, and the members of the Ginzton Lab for their guidance and help with this project. I would also like to thank Hugh Radkins, Jim Warner, Jeff Kissel, and Robert Schofield for their support at LIGO Hanford. Funding was provided by the Physics Summer Research Program in association with the Stanford Physics Department.

References

1. LIGO Caltech, "A Gravitational-Wave Interferometer," https://www.ligo.caltech.edu/.
2. LIGO Scientific Collaboration, "Instrument Science White Paper," *LIGO Document: LIGO-T1400316*, 2015. https://dcc.ligo.org/DocDB/0113/T1400316/004/T1400316-v5.pdf.
3. Lantz, B., R. Schofield, B. O'Reilly, D. E. Clark, and D. DeBra, "Requirements for a Ground Rotation Sensor to Improve Advanced LIGO," *Bulletin of the Seismological Society of America*, **99**, pp 980-989, 2009, http://dx.doi.org/10.1785/0120080199.
4. Vidrio, M. and R Schofield, "Statistics for 8 Years of Wind at LHO," *aLIGO LHO Logbook*, 2014, https://alog.ligo-wa.caltech.edu/aLOG/index.php?callRep=12996.
5. Schofield, R. and D. Talukder, "EY tilts twice as much as EX along the beam line, according to 4 months of seismometer data in the 0.03-0.08 Hz band," *aLIGO LHO Logbook*, 2015, https://alog.ligo-wa.caltech.edu/aLOG/index.php?callRep=17574.
6. Sumner, J. and C. Masson, "k-ε Simulations of the Neutral ABL: Achieving Horizontal Homogeneity on Practical Grid," *48th AIAA Aerospace Sciences Meeting Including the New Horizons Forum and Aerospace Exposition*, 2010, http://highorder.berkeley.edu/proceedings/aiaa-annual-2010/paper1106.pdf.
7. ANSYS Fluent, "Porous Jump Boundary Conditions," *Fluent Inc.*, 2006, https://www.sharcnet.ca/Software/Fluent6/html/ug/node288.htm.
8. Guo, L. and R.G. Maghirang, "Numerical Simulation of Airflow and Particle Collection by Vegetative Barriers," *Engineering Applications of Computational Fluid Mechanics*, **6**, pp 110-122, https://doi.org/10.1080/19942060.2012.11015407.